Contribution from the Department of Chemistry, University of Florence, Florence, Italy, Departement de Recherche Fondamentale, CEN, Grenoble, France, and Institut d'Electronique Fondamentale, Orsay, France

# Ferromagnetic Phase Transitions of Two One-Dimensional Ferrimagnets Formed by Manganese(II) and Nitronyl Nitroxides Cis Octahedrally Coordinated

Andrea Caneschi,[1a] Dante Gatteschi,*[1a] Jean Pierre Renard,[1b] Paul Rey,*[1c] and Roberta Sessoli[1a]

*Received January 9, 1989*

We report the structure of two chain compounds formed by manganese(II) hexafluoroacetylacetonate and nitronyl nitroxide radicals 2-R-4,4,5,5-tetramethyl-4,5-dihydro-1*H*-imidazolyl-1-oxy 3-oxide, $Mn(hfac)_2NITR$, with R ethyl, Et (I), and *n*-propyl, *n*-Pr (II), which crystallize in the monoclinic $P2_1/n$ space group with $a = 8.890$ (3) Å, $b = 25.573$ (5) Å, $c = 12.208$ (9) Å, $\beta = 103.52$ (5)°, and $Z = 4$ for I and $a = 9.297$ (6) Å, $b = 25.367$ (7) Å, $c = 12.215$ (4) Å, $\beta = 104.38$ (5)°, and $Z = 4$ for II. In both cases $Mn(hfac)_2$ units are bridged by NITR radicals which are cis-coordinated toward the manganese originating a zigzag chain. The magnetic susceptibility in the range of temperature 18-300 K is typical of a ferrimagnetic chain formed by alternating spins $^5/_2$ and spins $^1/_2$. The antiferromagnetic coupling constant has been estimated to be on the order of 260 $cm^{-1}$ for both compounds. Low-field magnetic measurements reveal that both compounds undergo a magnetic phase transition at 8.1 and 8.6 K for I and II, respectively. The magnetization curves indicate that the transition is ferromagnetic. The magnetic anisotropy, which is of the Ising type, is originated mainly by the dipolar interaction between manganese and radical. The EPR spectra at room temperature do not show the typical behavior of one-dimensional systems due to the fact that the chains are not linear but zigzag; however, effects due to short-range order are visible in the EPR resonance fields on lowering the temperature.

## Introduction

Low-dimensional magnetic materials are currently actively investigated, both as interesting research objects on their own[2-8] and also as intermediate building blocks in order to synthesize bulk molecular-based magnets.[9-13]

We have recently synthesized a few one-dimensional magnetic materials assembling metal hexafluoroacetylacetonates, $M(hfac)_2$, and nitronyl nitroxides, 2-R-4,4,5,5-tetramethyl-4,5-dihydro-1*H*-imidazolyl-1-oxy 3-oxide, NITR, whose general formula is

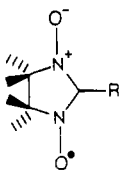

The general formula of these compounds is $M(hfac)_2NITR$, and when M = Cu ferromagnetic chains are formed,[14] while when M = Ni, Co, and Mn, the chains are ferrimagnetic.[15,16] While the one-dimensional ferromagnets do not undergo magnetic phase transitions above 1 K,[17] $Mn(hfac)_2NIT$-*i*-Pr, *i*-Pr = isopropyl (III), has been found to order ferromagnetically at 7.6 K.[18]

**Table I.** Crystallographic Data and Experimental Parameters for $Mn(hfac)_2NITEt$ (I) and $Mn(hfac)_2NIT$-*n*-Pr (II)

| | I | II |
|---|---|---|
| formula | $C_{19}H_{19}N_2O_6F_{12}Mn$ | $C_{20}H_{21}N_2O_6F_{12}Mn$ |
| mol wt | 654.3 | 668.3 |
| $a$, Å | 8.890 (3) | 9.297 (6) |
| $b$, Å | 25.573 (5) | 25.367 (7) |
| $c$, Å | 12.208 (9) | 12.215 (4) |
| $\beta$, deg | 103.52 (5) | 104.38 (5) |
| $V$, Å$^3$ | 2698.5 | 2790.5 |
| $Z$ | 4 | 4 |
| space group | $P2_1/n$ (No. 14) | $P2_1/n$ (No. 14) |
| density, g/cm$^3$ | 1.610 | 1.591 |
| $\mu$, cm$^{-1}$ | 5.46 | 5.29 |
| temp, °C | 20 | 20 |
| $\lambda$ (Mo K$\alpha$), Å | 0.7107 | 0.7107 |
| refinement | $R = 0.077$ | $R = 0.079$ |
| | $R_w = 0.077$ | $R_w = 0.079$ |

In $Mn(hfac)_2NIT$-*i*-Pr the metal ion is octahedrally coordinated and the oxygen atoms of two different radicals occupy two sites trans to each other. The chains are fairly well shielded from each other, in such a way that this compound has been suggested to be an ideal one-dimensional ferrimagnet.[15,18]

We have also synthesized $Mn(hfac)_2NITEt$ (I) and $Mn(hfac)_2NIT$-*n*-Pr (II), which have high temperature magnetic properties very close to those of the isopropyl derivative (III). On this basis,[15] we suggested a chain structure also for the former. However we have now found that in I and II the radicals bind in a cis configuration around the octahedral manganese ions. Therefore, we wish to report here the crystal structure, the EPR spectra, and the magnetic phase transitions of I and II and to compare these with those of III in order to determine if, and how, a difference in coordination can affect the magnetic properties of this class of one-dimensional materials.

## Experimental Section

**Synthesis of the Complexes.** $Mn(hfac)_2NITEt$ (I) was synthesized as previously reported.[15] The synthesis of $Mn(hfac)_2NIT$-*n*-Pr (II) is substantially similar: both $Mn(hfac)_2{\cdot}2H_2O$ and NIT-*n*-Pr were prepared as previously described.[19-21] The complex $Mn(hfac)_2NIT$-*n*-Pr was obtained by dissolving 0.5 mmol of $Mn(hfac)_2{\cdot}2H_2O$ in 30 mL of boiling *n*-heptane and then adding 0.5 mmol of NIT-*n*-Pr dissolved in 15 mL of warm *n*-heptane. The solution was allowed to cool down to room temperature, and then it was stored at 4 °C for 12 h. Wine red crystals suitable for X-ray diffraction analysis were collected. The compound analyzed satisfactorily for $Mn(hfac)_2NIT$-*n*-Pr. Anal. Calcd for

(1) (a) University of Florence. (b) Institut d'Electronique Fondamentale. (c) CEN.
(2) Miller, J. S.; Epstein, A. J. *Prog. Inorg. Chem.* **1976**, *20*, 1.
(3) de Jongh, L. J.; Miedema, A. R. *Adv. Phys.* **1974**, *23*, 1.
(4) de Jongh, L. J. *J. Appl. Phys.* **1982**, *53*, 8018.
(5) Hoogerbeets, R.; Wiegers, S. A. J.; van Duyneveldt, A. J.; Willett, R. D.; Geiser, U. *Physica B+C* **1984**, *125*, 135.
(6) Geiser, U.; Willett, R. D.; Lindbeck, M.; Emerson, K. *J. Am. Chem. Soc.* **1986**, *108*, 1173.
(7) Landee, C. P. In *Organic and Inorganic Low Dimensional Crystalline Materials*; Delhaes, P., Drillon, M., Eds.; NATO ASI SERIES; Plenum: New York, 1987.
(8) Coronado, E.; Barba, A.; Beltran, D.; Burriel, R.; Carlin, R. in *Organic and Inorganic Low Dimensional Crystalline Materials*; Delhaes, P., Drillon, M., Eds.; NATO ASI SERIES; Plenum: New York, 1987.
(9) Miller, J. S.; Epstein, A. J.; Reiff, W. M. *Chem. Rev.* **1988**, *88*, 201.
(10) Kahn, O. In *Organic and Inorganic Low Dimensional Crystalline Materials*; Delhaes, P., Drillon, M., Eds.; NATO ASI SERIES; Plenum: New York, 1987.
(11) Sugawara, T.; Bandow, S.; Kimura, K.; Iwamura, H.; Itoh, K. *J. Am. Chem. Soc.* **1986**, *108*, 368.
(12) Georges, R.; Curély, J. Drillon, M. *J. Appl. Phys.* **1985**, *58*, 914.
(13) Coronado, E.; Drillon, M.; Fuertes, A.; Beltran, D.; Mosset, A.; Galy, J. *J. Am. Chem. Soc.* **1986**, *108*, 900.
(14) Caneschi, A.; Gatteschi, D.; Laugier, J.; Rey, P. *J. Am. Chem. Soc.* **1987**, *109*, 2191.
(15) Caneschi, A.; Gatteschi, D.; Renard, J. P.; Rey, P.; Sessoli, R. *Inorg. Chem.* **1989**, *28*, 2940.
(16) Caneschi, A.; Gatteschi, D.; Rey, P.; Sessoli, R. *Inorg. Chem.* **1988**, *27*, 1786.
(17) Unpublished results of the Florence laboratory.
(18) Caneschi, A.; Gatteschi, D.; Renard, J. P.; Rey, P.; Sessoli, R. *Inorg. Chem.* **1989**, *28*, 1976.
(19) Cotton, F. A.; Holm, R. H. *J. Am. Chem. Soc.* **1960**, *86*, 2979.
(20) Ullman, E. F.; Call, L.; Osiecky, J. H. *J. Org. Chem.* **1970**, *35*, 3623.
(21) Ullman, E. F.; Osiecky, J. H.; Boocock, D. G. B.; Darcy, R. *J. Am. Chem. Soc.* **1972**, *94*, 7049.

0020-1669/89/1328-3314$01.50/0 

**Table II.** Positional Parameters and Isotropic Thermal Factors ($Å^2 \times 10^3$) for $Mn(hfac)_2NITEt$[a]

| | $x$ | $y$ | $z$ | $U_{eq}$ |
|---|---|---|---|---|
| Mn | 0.2380 (3) | 0.3331 (1) | 0.2544 (2) | 55 |
| O1 | 0.0153 (11) | 0.3693 (4) | 0.1915 (7) | 76 |
| O2 | 0.1953 (10) | 0.3571 (3) | 0.4124 (7) | 60 |
| O3 | 0.2815 (10) | 0.3330 (3) | 0.0889 (6) | 62 |
| O4 | 0.3338 (10) | 0.4108 (3) | 0.2565 (7) | 66 |
| O5 | 0.4452 (10) | 0.2976 (3) | 0.3485 (6) | 68 |
| O6 | 0.6286 (9) | 0.2416 (3) | 0.7151 (6) | 55 |
| N1 | 0.5219 (11) | 0.2962 (4) | 0.4518 (8) | 45 |
| N2 | 0.6156 (11) | 0.2682 (4) | 0.6227 (8) | 44 |
| C1 | −0.0345 (16) | 0.4074 (6) | 0.2323 (12) | 63 |
| C2 | 0.1254 (16) | 0.3977 (6) | 0.4266 (12) | 61 |
| C3 | 0.0115 (16) | 0.4240 (6) | 0.3443 (12) | 78 |
| C4 | −0.171 (3) | 0.4364 (12) | 0.1622 (20) | 128 |
| C5 | 0.166 (3) | 0.4225 (9) | 0.5403 (15) | 97 |
| C6 | 0.2999 (16) | 0.3719 (6) | 0.0332 (12) | 65 |
| C7 | 0.3413 (15) | 0.4392 (5) | 0.1774 (12) | 56 |
| C8 | 0.3262 (16) | 0.4248 (6) | 0.0662 (13) | 73 |
| C9 | 0.278 (4) | 0.3610 (10) | −0.0915 (17) | 145 |
| C10 | 0.372 (3) | 0.4960 (7) | 0.2094 (19) | 102 |
| C11 | 0.5008 (14) | 0.2625 (4) | 0.5267 (10) | 45 |
| C12 | 0.6725 (15) | 0.3269 (5) | 0.4863 (11) | 57 |
| C13 | 0.2173 (14) | 0.1859 (5) | 0.1121 (10) | 52 |
| C14 | 0.3708 (15) | 0.2248 (5) | 0.5151 (11) | 62 |
| C15 | 0.2595 (19) | 0.2398 (7) | 0.5840 (14) | 102 |
| C16 | 0.6389 (19) | 0.3840 (5) | 0.4584 (13) | 99 |
| C17 | 0.7810 (18) | 0.3043 (7) | 0.4206 (14) | 105 |
| C18 | 0.8862 (15) | 0.2972 (7) | 0.6602 (14) | 115 |
| C19 | 0.666 (2) | 0.3550 (6) | 0.6923 (14) | 110 |
| F1 | −0.2778 (19) | 0.4079 (7) | 0.118 (3) | 280 |
| F2 | −0.2192 (25) | 0.4750 (7) | 0.1963 (15) | 269 |
| F3 | −0.128 (2) | 0.4512 (10) | 0.0704 (20) | 257 |
| F4 | 0.0501 (16) | 0.4312 (7) | 0.5838 (11) | 186 |
| F5 | 0.255 (2) | 0.3953 (8) | 0.6108 (10) | 273 |
| F6 | 0.226 (2) | 0.4659 (8) | 0.5454 (12) | 235 |
| F7 | 0.1753 (16) | 0.3278 (6) | −0.1322 (8) | 170 |
| F8 | 0.405 (2) | 0.3310 (9) | −0.1010 (13) | 204 |
| F9 | 0.284 (3) | 0.3993 (5) | −0.1524 (9) | 247 |
| F10 | 0.2432 (19) | 0.5189 (4) | 0.2079 (17) | 189 |
| F11 | 0.4217 (17) | 0.5235 (4) | 0.1322 (11) | 156 |
| F12 | 0.4621 (20) | 0.5041 (4) | 0.2985 (11) | 209 |

[a] Standard deviations in the last significant digit are given in parentheses.

$C_{20}F_{12}H_{21}MnN_2O_6$: C, 35.93; H, 3.14; N, 4.19. Found: C, 35.81; H, 3.23; N, 4.08.

**X-ray Analysis.** Diffraction data were collected for compounds I and II at room temperature on a ENRAF Nonius CAD4 four-circle diffractometer equipped with Mo K$\alpha$ radiation and a graphite crystal monochromator. The habit of the crystals of both compounds is that of elongated platelets. Unit cell parameters were determined by least-squares refinement of 20 reflections ($8 \le \theta \le 15°$). Data were corrected for Lorentz and polarization effects, but not for absorption and extinction. More details are given in Table SI in the supplementary material while an abbreviation version is given in Table I. The systematic extinctions revealed that both compounds belong to the monoclinic system, space group $P2_1/n$. The position of the manganese atom was revealed in both cases by direct methods, performed by using the MULTAN77 package,[22] while the other non-hydrogen atoms were revealed by successive difference Fourier synthesis using a standard program.[23] Some difficulties were met in the refinement procedure of both structures due to disorder and/or pronounced anisotropic thermal motion present in the $CF_3$ groups of the hexafluoroacetylacetonate moieties. In the case of the NITEt derivative (I) no model of disorder was used. Even if the geometry of the $CF_3$ groups was correct, large and very anisotropic thermal ellipsoids were observed for the fluorine and the carbon atoms. Due to the small number of reflections with $F \ge 3\sigma(F)$ only manganese, oxygen, fluorine, and eight carbon atoms were anisotropically refined. The hydrogen atoms were introduced in fixed and idealized positions with thermal factors about 10% greater than that of the respective carbon atom. The final agreement factor was $R = 0.077$ and the highest peaks of the final difference Fourier map were about 0.5 e/Å$^3$ and placed near the fluorine atoms.

A more evident disorder was found in the $CF_3$ groups of II and the model adopted considered the F1–F2–F3 and F7–F8–F9 groups twice with an occupation factor of 0.5, while for F4–F5–F6 the occupation factors were 0.7 and 0.3. No remarkable disorder was found in the F10–F11–F12 group. The geometry of the groups was correct, but the uncertainty in the positions of the disordered fluorine atoms was very large and a significant correlation of the parameters was present. Nevertheless, the disorder did not affect seriously the precision of the structural results, especially in the manganese environment, and the final refinement including the fixed contribution of hydrogen atoms converged to $R = 0.079$. The highest peaks in the last difference Fourier map were about 0.6 e/Å$^3$. The atomic coordinates and isotropic thermal factors are reported in Tables II and III for I and II, respectively. Anisotropic thermal factors and hydrogen coordinates are available as supplementary material (Tables SII–SV), as well as observed and calculated structure factors for I and II.

**EPR and Magnetic Measurements.** Variable-temperature EPR spectra, in the range 4.2–300 K, were recorder with a Bruker ER200 spectrometer operating at X-band frequency and equipped with an Oxford Instruments ESR90 continuous-flow cryostat. The crystals used in single-crystal EPR and magnetic measurements were oriented by using the same diffractometer mentioned above. The crystals of both compounds have largely developed (010) and (0$\bar{1}$0) faces and are elongated along the (101) direction.

The magnetic susceptibility of II in the range 6–300 K was measured with an SHE SQUID susceptometer at field strength of 100 Oe. Data were corrected for the magnetization of the sample holder and for the diamagnetic contributions, which were estimated from Pascal's constants.

The magnetic susceptibility of single crystals of I and II glued on monocrystalline platelets of silicon was measured with a low-field operating SQUID magnetometer[24] in the temperature range 1.8–12 K and with the magnetic field ranging from 0 to 1 Oe. The different experi-

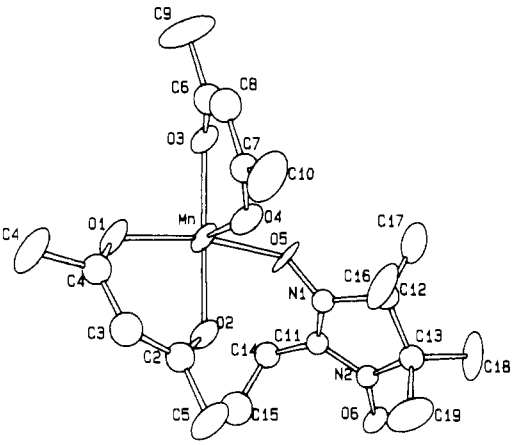


**Figure 1.** ORTEP view of $Mn(hfac)_2NITEt$. The fluorine atoms were omitted for the sake of clarity.

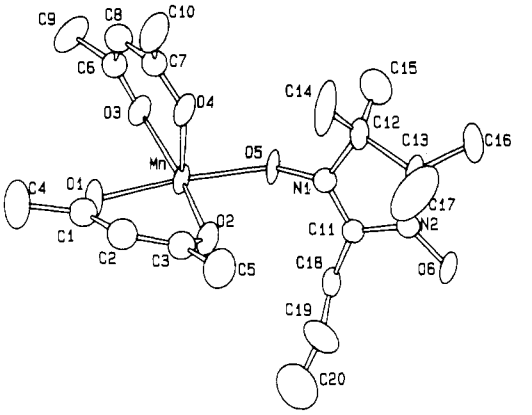


**Figure 2.** ORTEP view of $Mn(hfac)_2NIT$-*n*-Pr. The fluorine atoms were omitted for the sake of clarity.

(22) Main, P.; Woolfson, M. M.; Germain, G. "MULTAN 77 Direct Methods Program".

(23) Sheldrick, G. "SHELX76 System of Computing Programs", University of Cambridge, Cambridge, England, 1976. Atomic scattering factors are after: Cromer, D. T.; Lieberman, D. *J. Chem. Phys.* **1970**, *53*, 1891.

(24) Beauvillain, P.; Chappert, C.; Renard, J. P. *J. Phys. E* **1985**, *18*, 839.

**Table III.** Positional Parameters and Isotropic Thermal Factors ($Å^2 \times 10^3$) for $Mn(hfac)_2NIT$-*n*-Pr[a]

| | *x* | *y* | *z* | $U_{eq}$ |
|---|---|---|---|---|
| Mn | 0.2468 (1) | 0.3337 (1) | 0.2515 (1) | 53 |
| O1 | 0.0389 (6) | 0.3752 (2) | 0.1814 (4) | 80 |
| O2 | 0.1998 (6) | 0.3574 (2) | 0.4062 (3) | 68 |
| O3 | 0.2755 (5) | 0.3313 (2) | 0.0832 (3) | 62 |
| O4 | 0.3507 (6) | 0.4088 (2) | 0.2532 (3) | 69 |
| O5 | 0.4489 (5) | 0.2985 (2) | 0.3474 (3) | 65 |
| O6 | 0.6378 (5) | 0.2411 (2) | 0.7145 (3) | 60 |
| N1 | 0.5284 (6) | 0.2976 (2) | 0.4534 (4) | 51 |
| N2 | 0.6222 (6) | 0.2696 (2) | 0.6237 (4) | 48 |
| C1 | −0.0079 (9) | 0.4122 (3) | 0.2259 (7) | 72 |
| C2 | 0.1319 (9) | 0.3973 (3) | 0.4203 (6) | 69 |
| C3 | 0.0302 (10) | 0.4274 (4) | 0.3406 (7) | 83 |
| C4 | −0.129 (2) | 0.4470 (7) | 0.1441 (16) | 130 |
| C5 | 0.1656 (12) | 0.4191 (4) | 0.5433 (7) | 105 |
| C6 | 0.2933 (8) | 0.3707 (3) | 0.0256 (6) | 58 |
| C7 | 0.3618 (8) | 0.4371 (3) | 0.1726 (6) | 59 |
| C8 | 0.3348 (8) | 0.4211 (3) | 0.0580 (7) | 71 |
| C9 | 0.2596 (13) | 0.3594 (4) | −0.1032 (6) | 106 |
| C10 | 0.4007 (13) | 0.4929 (3) | 0.1986 (8) | 107 |
| C11 | 0.5081 (7) | 0.2618 (2) | 0.5273 (5) | 46 |
| C12 | 0.6638 (9) | 0.3316 (3) | 0.4897 (6) | 77 |
| C13 | 0.7118 (9) | 0.3161 (3) | 0.6178 (6) | 71 |
| C14 | 0.6298 (14) | 0.3865 (4) | 0.4635 (9) | 174 |
| C15 | 0.7745 (12) | 0.3086 (6) | 0.4255 (9) | 144 |
| C16 | 0.8744 (10) | 0.3022 (4) | 0.6598 (9) | 140 |
| C17 | 0.6724 (18) | 0.3560 (4) | 0.6957 (9) | 181 |
| C18 | 0.3908 (8) | 0.2233 (3) | 0.5137 (6) | 71 |
| C19 | 0.2826 (12) | 0.2371 (5) | 0.5873 (12) | 134 |
| C20 | 0.1625 (16) | 0.2030 (7) | 0.5727 (14) | 219 |
| F1a | −0.115 (8) | 0.4947 (16) | 0.174 (5) | 262 |
| F2a | −0.125 (6) | 0.441 (2) | 0.0454 (20) | 164 |
| F3a | −0.258 (3) | 0.431 (2) | 0.158 (4) | 203 |
| F1b | −0.184 (8) | 0.480 (3) | 0.192 (4) | 263 |
| F2b | −0.057 (4) | 0.476 (3) | 0.080 (7) | 274 |
| F3b | −0.220 (9) | 0.4196 (16) | 0.076 (7) | 269 |
| F4a | 0.0499 (19) | 0.4331 (9) | 0.5717 (11) | 144 |
| F5a | 0.215 (4) | 0.3818 (11) | 0.6137 (10) | 218 |
| F6a | 0.251 (5) | 0.4568 (17) | 0.5569 (20) | 272 |
| F4b | 0.092 (2) | 0.392 (4) | 0.597 (3) | 374 |
| F5b | 0.158 (6) | 0.4700 (13) | 0.545 (4) | 148 |
| F6b | 0.304 (3) | 0.4127 (17) | 0.600 (3) | 101 |
| F7a | 0.200 (6) | 0.3168 (11) | −0.1330 (16) | 132 |
| F8a | 0.370 (4) | 0.366 (3) | −0.1444 (19) | 219 |
| F9a | 0.147 (6) | 0.3909 (17) | −0.1600 (17) | 188 |
| F7b | 0.357 (5) | 0.3233 (14) | −0.1189 (17) | 160 |
| F8b | 0.133 (4) | 0.337 (3) | −0.133 (2) | 208 |
| F9b | 0.280 (6) | 0.3998 (11) | −0.1605 (15) | 152 |
| F10 | 0.4383 (10) | 0.5208 (3) | 0.1209 (6) | 165 |
| F11 | 0.5066 (11) | 0.4985 (3) | 0.02861 (6) | 238 |
| F12 | 0.2883 (11) | 0.5200 (3) | 0.2153 (10) | 203 |

[a] Standard deviations in the last significant digit are given in parentheses.

mental procedures employed, as field-cooling and zero-field-cooling measurements, were already described in previous papers.[15,25]

Hysteresis loops were recorded at 4.2 and 1.2 K for powdered samples of both I and II and on a single-crystal of I by using a conventional fluxmetric method.

## Results

**Crystal Structure.** The structures of $Mn(hfac)_2NITEt$ and $Mn(hfac)_2NIT$-*n*-Pr are very similar to each other and consist of chains of $Mn(hfac)_2$ units bridged by NITR radicals. The asymmetric unit comprises a $Mn(hfac)_2NITR$ group and is shown in Figures 1 and 2 for I and II, respectively. In both compounds, the manganese ion is hexacoordinated by four oxygen atoms belonging to two hfac molecules and two oxygen atoms belonging to two different radicals. The other oxygens of the two radicals are coordinated to the two adjacent manganese ions. The main difference from the structure of $Mn(hfac)_2NIT$-*i*-Pr previously reported is that in the present case the two radicals are cis coordinated around manganese. A similar difference in coordination was previously observed also in mononuclear manganese(II)–nitroxide complexes, where $Mn(hfac)_2(NITPh)_2$ has a trans and $Mn(hfac)_2(NITMe)_2$ has a cis coordination.[26] A cis coordination was observed also in the hexanuclear cluster $[Mn(hfac)_2NITPh]_6$, which has a ring structure.[27]

**Table IV.** Selected Bond Lengths (Å) for $Mn(hfac)_2NITEt$ (I) and $Mn(hfac)_2NIT$-*n*-Pr (II)[a]

| | I | II |
|---|---|---|
| Mn–O1 | 2.157 (9) | 2.182 (5) |
| Mn–O2 | 2.141 (9) | 2.129 (5) |
| Mn–O3 | 2.144 (9) | 2.138 (4) |
| Mn–O4 | 2.160 (9) | 2.135 (5) |
| Mn–O5 | 2.133 (8) | 2.146 (4) |
| Mn–O6′ | 2.147 (8) | 2.146 (4) |
| O5–N1 | 1.287 (11) | 1.322 (6) |
| O6–N2 | 1.299 (12) | 1.301 (7) |

[a] Standard deviations in the last significant digit are in parentheses.

**Table V.** Bond Angles (deg) for $Mn(hfac)_2NITEt$ (I) and $Mn(hfac)_2NIT$-*n*-Pr (II)[a]

| | I | II |
|---|---|---|
| O1–Mn–O2 | 81.7 (3) | 81.6 (2) |
| O1–Mn–O3 | 91.0 (3) | 86.9 (2) |
| O1–Mn–O4 | 86.4 (3) | 85.8 (2) |
| O1–Mn–O5 | 168.4 (3) | 170.3 (2) |
| O1–Mn–O6′ | 88.4 (3) | 91.0 (2) |
| O2–Mn–O3 | 163.4 (3) | 164.4 (2) |
| O2–Mn–O4 | 83.0 (3) | 86.1 (2) |
| O2–Mn–O5 | 87.1 (3) | 88.7 (2) |
| O2–Mn–O6′ | 87.9 (3) | 104.3 (2) |
| O3–Mn–O4 | 81.7 (3) | 82.6 (2) |
| O3–Mn–O5 | 100.6 (3) | 102.2 (2) |
| O3–Mn–O6′ | 87.9 (3) | 86.4 (2) |
| O4–Mn–O5 | 95.6 (3) | 91.9 (2) |
| O4–Mn–O6′ | 168.1 (3) | 168.6 (2) |
| O5–Mn–O6′ | 91.8 (3) | 92.9 (2) |

[a] Standard deviations in the last significant digit are given in parentheses.

The Mn–O distances are almost constant in both compounds, ranging from 2.133 (8) to 2.160 (9) Å and from 2.129 (5) to 2.182 (5) Å for I and II, respectively, as can be seen in Tables IV and V where selected bond distances and angles are reported. All bond distances and angles are available as supplementary material. The coordination octahedron is severely distorted in both cases, probably in order to release steric hindrance between the hfac molecules and the nitroxides. In both compounds the two Mn–O–N angles are different from each other: 137.1 (7) vs 126.9 (7)° for I and 137.9 (4) vs 128.1 (4)° for II. These angles, as well as the N–O distances, compare well with those reported for other coordinated NITR radicals.[14-16,26,27] The distances and angles within the radicals are fairly normal.[28] The five-membered ring is almost planar in both cases with the carbon atoms carrying the methyl groups displaced by 0.9 and 0.8 Å from the average plane for I and II, respectively. The average plane containing the conjugate group O–N–C–N–O is almost orthogonal to the Mn–O–N planes for both compounds: 85.2 and 83.0° for I; 87.6 and 83.0° for II.

The chains develop along the [101] direction with two nearest-neighbor units related by the *n* glide plane. In Figure 3, we report a simplified view of the content of two cells of $Mn(hfac)_2NITEt$ sharing an edge. Every chain is surrounded by eight nearest-neighbor chains at distances, calculated as manganese–manganese contacts, ranging from 8.89 to 12.11 Å. The crystal structure of II is practically identical.

(25) Kahn, O.; Pei, Y.; Verdaguer, M.; Renard, J. P.; Sletten, J. *J. Am. Chem. Soc.* **1988**, *18*, 839.

(26) Caneschi, A.; Gatteschi, D.; Laugier, J.; Pardi, L.; Rey, P.; Zanchini, C. *Inorg. Chem.* **1988**, *27*, 2027.

(27) Caneschi, A.; Gatteschi, D.; Laugier, J.; Rey, P.; Sessoli; R.; Zanchini, C. *J. Am. Chem. Soc.* **1988**, *110*, 2795.

(28) Wong, W. H.; Watkins, S. F. *J. Chem. Soc., Chem. Commun.* **1973**, 888.

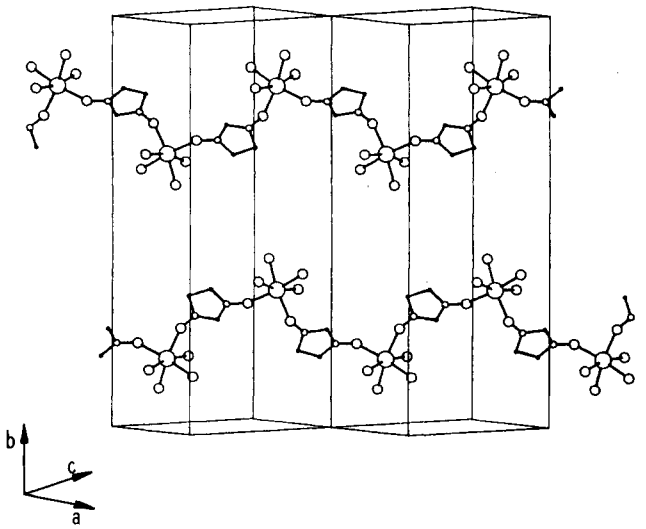


**Figure 3.** Schematic view of the content of two unit cells of I sharing an edge. The circles in order of decreasing dimension represent the manganese, oxygen, nitrogen, and carbon atoms.

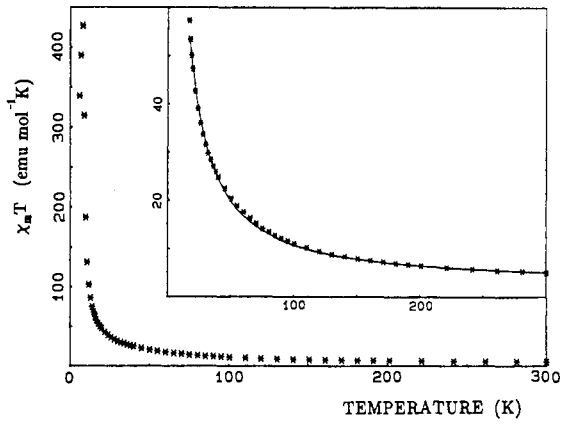


**Figure 4.** $\chi T$ vs $T$ for Mn(hfac)$_2$NIT-*n*-Pr. In the inset the solid line represents the best fit (see text).

**Magnetic Properties.** The temperature dependence of $\chi T$ of II is shown in Figure 4. The room-temperature value is 5.1 emu mol$^{-1}$ K and increases on decreasing temperature; below 10 K a very sharp increase is observed with a maximum of about 427 emu mol$^{-1}$ K. This behavior is similar to that observed for I and other linear-chain compounds of formula Mn(hfac)$_2$NITR, which have been considered as infinite arrays of alternating spins $^5/_2$ and spins $^1/_2$ antiferromagnetically coupled.[15] The quantitative analysis of the magnetic susceptibility of II was performed by using a model that considers the manganese spin as a classical vector but takes into account the quantic nature of the spin of the radical.[29] From the fitting of the experimental data we obtained an antiferromagnetic coupling constant $J$ = 258.3 (2) cm$^{-1}$, with the hamiltonian written in the form $H = J\sum_{i\leq j} S_i S_j$ and the $g$ value taken equal to 2 for both the manganese and the radical. The same model was previously used with other manganese-radical chains, and in particular, for the NITEt derivative I we obtained $J$ = 259.5.[15] The calculated $\chi T$ products are in good agreement with the experimental ones, as can be seen in Figure 4. The points below 18 K cannot be reproduced with this model due to the occurrence of a magnetic phase transition.

The single-crystal susceptibility was measured in low field for both compounds along the [101] ($z$) and the [010] ($y$) directions and along a third axis perpendicular to these ($x$). The experimental values for I are shown in Figure 5. The data show that a magnetic phase transition occurs for Mn(hfac)$_2$NITEt at about 8.1 K. The anisotropy is of the Ising type with a preferred spin

(29) Seiden, J. *J. Phys., Lett.* **1983**, *44*, L947.

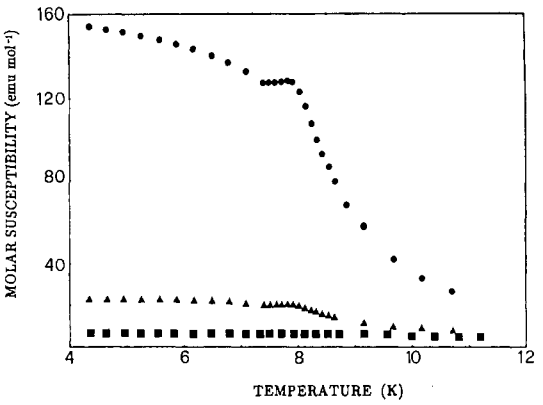


**Figure 5.** Magnetic susceptibility measured on an oriented crystal of I in an external magnetic field of 0.5 Oe parallel to the $x$ (●), $y$ (■), and $z$ (▲) axes.

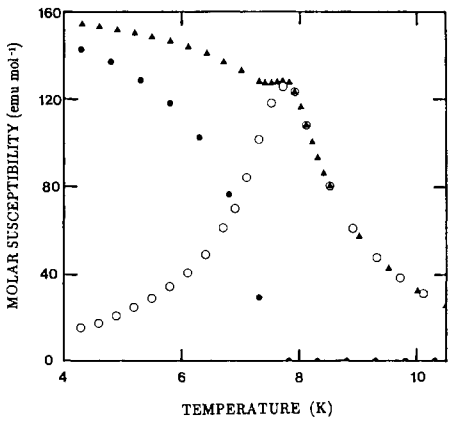


**Figure 6.** Field-cooled (▲) and zero-field-cooled (○) susceptibility and remnant magnetization (●), divided by the cooling field of 0.5 Oe, along the $x$ axis of I.

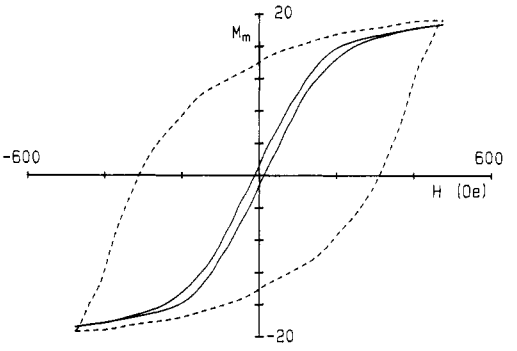


**Figure 7.** Hysteresis loops of I with the applied magnetic field parallel to the $x$ axis at two temperatures: solid line, $T$ = 4.2 K; dashed line, $T$ = 1.25 K. The molar magnetization is given in (emu mol$^{-1}$ G)/10$^3$.

orientation parallel to the $x$ direction and two hard axes, with the $z$ direction having a higher susceptibility than the $y$ one. The susceptibility along the easy axis reaches a plateau as expected due to demagnetizing effects. The demagnetizing factor evaluated from the value at the plateau is $n_x$ = 3.1 and is in agreement with the shape of the crystal. The other two demagnetizing factors were roughly estimated to be $n_y$ = 8 and $n_z$ = 1.5.

Below 7.5 K the susceptibility along the $x$ direction begins to increase again. The measurements performed by cooling the sample in zero field (ZFC) and then switching on the field reveal a large irreversibility below 7.8 K as shown for I in Figure 6. In fact the ZFC susceptibility at 4.2 K is 16.2 emu mol$^{-1}$, against 154.2 emu mol$^{-1}$ for the FC experiment, and increases when the temperature is increased up to 7.8 K where the two curves become superimposable. In order to determine the origin of this behavior, we performed accurate measurements of the magnetization of I along the $x$ axis in the range of temperature 1.8–8 K in two

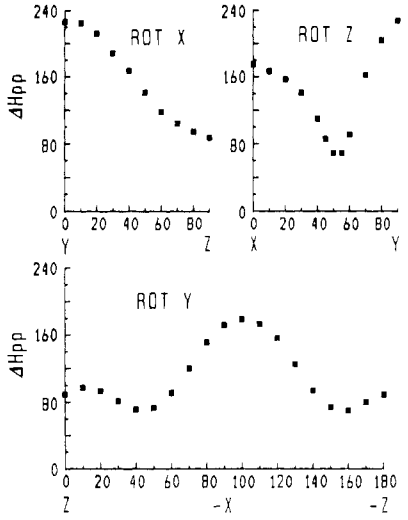


**Figure 8.** Angular dependence of the line width of the EPR line of I at X-band frequency and room temperature in the rotations along the $x$, $y$, and $x$ axes.

different magnetic fields, 0.1 and 1 Oe. In both cases, the magnetization, in the form $M(0) - M(T)$, was proportional to $T^{3/2}$ below 5 K.

The hysteresis loop on the powder sample shows that the magnetization in the maximum field available, 460 Oe, is 10482 emu mol$^{-1}$ G, in agreement with the observed anisotropy. The results of the measurements on a single crystal of I are shown in Figure 7. Along the $x$ direction, the magnetization is 19375 emu mol$^{-1}$ G at a field strength of 460 Oe, which is the maximum available in our apparatus. At low temperature, the antiferromagnetic coupling between manganese and radicals yields an $S = 2$ state for a unit formula. If these spins order ferromagnetically, the saturation value is 22330 emu mol$^{-1}$ G, which is in good agreement with our experimental value obtained in a field not strong enough to completely saturate the magnetization. While the magnetization reached in the maximum field available did not change significantly in going from $T = 4.2$ to $T = 1.2$ K, the remnant magnetization and the coercitive field increase dramatically, lowering the temperature. At 1.2 K, the residual magnetization is about 70% of the value at 460 Oe but goes down to 6% at 4.2 K. Even at the lowest temperature, the remnant magnetization is not stable in time but decreases slowly, going asymptotically to zero.

The magnetic properties of II are practically identical with those of I. The observed transition temperature for the former is about 8.6 K.

**EPR Spectra.** At room temperature the EPR spectra of single crystals of both compounds show a single line centered at $g = 2$ for every field setting. In Figure 8 is shown the angular behavior of the line width for I in three different rotations along the $x$, $y$, and $x$ axes. The largest line width, 225 G, is observed along the $y$ axis. Rotating along the $x$ direction causes the line width to decrease steadily going from the $y$ direction to $z$, the chain direction, where the line width is 89 G. In the rotation along the $y$ direction the line width presents a magic-angle behavior along a direction that makes an angle of about 10° with the $x$ axis. The two symmetric minima have line widths of 70 G. Rotating along the $z$ axis gives a deep minimum at 55° from $x$, but the line width parallel to $x$, 175 G, is smaller than that observed parallel to $y$. The line shape is Lorentzian at all angular settings.

The spectra of II show the same behavior as those of I but the line widths are smaller. The values of the line widths along the $x$, $y$, and $z$ directions are 161, 200, and 75 G, respectively.

The EPR spectra of both compounds are temperature dependent. Lowering the temperature causes the line width to increase steadily while the resonance field moves depending on the field setting. Along the $x$ axis, the resonance moves downfield and goes upfield along the other two directions. As can be seen in Figure 9, the $g$ shifts of I show the same anisotropy observed

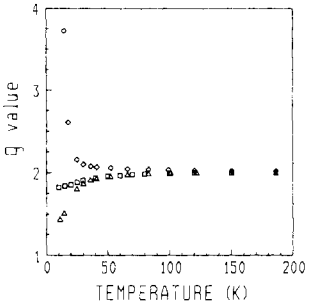


**Figure 9.** Temperature dependence of the experimental $g$ values observed at three different settings of the magnetic field: parallel to $x$ (◇), to $y$ (△), and to $z$ (□) axes.

in the magnetic measurements, the $x$ axis being the easy one and the $y$ axis the hardest one. The shifts becomes very large below 20 K where the spectra may be affected by the transition to the three-dimensional ordered state.

## Discussion

The high-temperature (18–300 K) magnetic susceptibility data of both I and II are in agreement with a ferrimagnetic chain. The best fit $J$ values, ca. 260 cm$^{-1}$, are slightly smaller than that found for III (320 cm$^{-1}$),[15] in which the chains are formed by nitroxides binding manganese(II) as trans adducts. On the other hand the best fit $J$ values of I and II are larger than the value reported for the mononuclear cis adduct $Mn(hfac)_2(NITMe)_2$ ($J$ = 187 cm$^{-1}$).[26] We previously observed that the quantic–classic treatment gives best fit values of the coupling constant that are much larger than the values found for mononuclear compounds where more accurate quantitative treatments are available, and the present results seem to confirm this observation.[15]

The substantial identity of the $J$ values for I and II agrees with the close similarity of the bond angles and distances around manganese. These geometrical parameters are rather similar also in the trans adduct so that the $J$ values would be expected to be very close to each other in I–III, but this is not the case. It seems therefore that accurate structural–magnetic correlations in these chain compounds are difficult to establish.

The high-temperature EPR data clearly indicate that I and II are far from the ideal one-dimensional ferrimagnetic behavior observed in III. In fact, we can expect to have ideal behavior when[30] (i) the main broadening mechanism of the EPR lines is given by intrachain dipolar interactions parallel to the chain direction and (ii) the interchain interactions are weak. The latter condition should be well obeyed in the present case, as shown by the long distances between the chains and the relatively low temperatures of the magnetic phase transitions. Condition i is not obeyed in the present case, because the main dipolar interaction is expected to be roughly parallel to the $Mn–O_{rad}$ directions, and these in cis chains make angles of about 90° with each other.

A quantitative treatment of the angular dependence of the line width was attempted, using only the dipolar interaction. The dipolar second moment was computed by using standard procedures,[31] calculating separately the secular and nonsecular terms. Since the manganese–manganese interactions have a large weight in the sum, we included not only the adjacent manganese ions along the chain but also the interactions with all the manganese ions contained in a sphere of radius 13.5 Å around the central one. The calculated line widths, including only the secular terms, bear some resemblance to the experimental data, reproducing for instance the two maxima in the rotation around $y$. However the relative height of the two maxima is not correctly given, inducing us to suspect that other broadening mechanisms can be also responsible for the line width. In fact, another possible broadening mechanism is provided by single-ion zero-field splitting, but since

(30) Richards, P. M. in *Local Properties at Phase Transitions*; Editrice Compositori: Bologna, Italy, 1975.
(31) Pake, G. E. *Paramagnetic Resonance*; W. A. Benjamin Inc.: New York, 1962.

the symmetry around manganese is so low and no independent information on the crystalline field effects is available, we did not pursue further this problem.

The $g$ shifts that were observed at low temperature are due to short-range order effects.[32] The $g$ shifts provide the preferred spin orientations and are expected to be determined by the nature of the intrachain exchange interaction and the magneto crystalline anisotropy. The $g$ shift has the same origin as the anisotropic magnetic susceptibility observed above the magnetic phase transition temperature. In fact, the resonance fields along the three principal axes can be expressed as

$$B_a = \left(\sqrt{\chi_b \chi_c}/\chi_a\right)(g_e/g_a)B_0$$

where $\chi_a$, $\chi_b$, and $\chi_c$ are the principal susceptibilities in the paramagnetic region, $g_a$ is the indicated principal $g$ value, $g_e$ = 2.0023, and $B_0$ is the resonance field of the free electron.[33,34] The resonance fields for the other principal directions follow from cyclic permutations.

The observed shifts compare well with the reported magnetic susceptibility data, which showed an anisotropy of the Ising type for both I and II, while in III the anisotropy is of the XY type. The origin of the difference is well understood on the basis of the structural differences. In fact, for ferrimagnetic chains, the preferred spin orientation is orthogonal to the direction of maximum dipolar interaction. In an ideal one-dimensional ferrimagnet, like III, the chain direction corresponds to the maximum dipolar interaction, so that the preferred spin orientation is in the plane orthogonal to the chain. In I and II, the main dipolar interactions are zigzag approximately in the $yz$ plane; therefore, we must expect that the preferred spin orientation is parallel to $x$, as experimentally observed. The fact that this simple interpretation, using only dipolar interaction, works well seems to indicate that indeed this is the largest contribution to the spin orientation.

In order to confirm this interpretation with a quantitative treatment, we calculated the dipolar energy with a procedure previously described.[18] The calculations were performed for three different spin orientations, $x$, $y$, and $z$, including all the spins within a sphere of 80 Å, corresponding to 5220 spins on the whole. The calculated energies per mole are $E^x_{dip}$ = −0.15 K, $E^y_{dip}$ = 0.06 K, and $E^z_{dip}$ = 0.09 K for I. The results for II are practically identical. The most favorite spin orientation is the $x$ direction, as was found in the magnetic measurements and EPR spectra, while the order of the other two directions is reversed compared to the experimental results. Additive contributions from single-ion zero-field splitting might justify this discrepancy.

The nature of the phase transitions is ferromagnetic, as revealed by the hysteresis loop measured on a single crystal of I, which shows that parallel to the easy axis the magnetization goes very close to the saturation limit for a ferromagnet of spin $S$ = 2 in a very small field. In fact, for a ferromagnet the saturation field along the easy axis is expected to be on the order of the product of the volume magnetization by the demagnetizing factor.[35] In the present case this corresponds to 430 Oe for I, a value that compares well with experiment. For II only, the hysteresis loops on powdered samples were measured, and they are found to be practically identical with those of I.

Since the chains are fairly well shielded and no obvious exchange pathway is present between them, it is probable that the origin of the ferromagnetic phase transition is the dipolar interaction. Similar conclusions were previously reached for III.

The critical temperature in the case of Heisenberg chains is related to the dipolar interaction according to the relation[36,37]

$$T_c \cong \xi(T_c)\,|E_{dip}|$$

where $\xi(T)$ is the correlation length. The correlation length can be roughly estimated from the value of the effective spin of a manganese–radical pair:

$$\xi(T) = \frac{\chi(T)}{\chi_c(T)}\,\frac{S+1}{S} - \frac{1}{S}$$

where $\chi$ is the susceptibility of the chain calculated by using the quantic–classic approach previously mentioned[29] and $\chi_c$ is the Curie susceptibility of a system with $S$ = 2. Again, we consider the spins of the radical and of the manganese as completely antiferromagnetically coupled at low temperature, yielding $S$ = 2. The calculated transition temperature assuming $J$ = 260 cm$^{-1}$ and $E_{dip}$ = −0.15 K is $T_c$ = 8.4 K, a value in good agreement with the experimental results. The same calculation performed on III, for which the intrachain coupling constant is larger (330 cm$^{-1}$) but the dipolar energy in the preferred spin orientation is smaller ($E_{dip}$ = −0.13 K), yields $T_c$ = 8.8 K, while the transition is observed at $T_c$ = 7.6 K.

Beyond the quantitative agreement, we rationalize the higher transition temperature observed for I and II compared to III, notwithstanding the smaller $J$ values, which yield a shorter correlation length for the former, due to the fact that the Ising type anisotropy yields a larger $|E_{dip}|$. Furthermore, the correlation length at the critical temperature can also be increased by the Ising type anisotropy. In fact it is well-known that $\xi_{Ising} > \xi_{XY} > \xi_{Heis}$ at a given temperature and for the same $J$ value.[36]

The two present compounds differ from III in their magnetic behavior at very low temperature. A large irreversibility of the susceptibility below the transition temperatures is observed for I and II, while it was not observed for III. The ZFC susceptibility of I and II is in fact much smaller than the FC susceptibility, and a large residual magnetization is present. The hysteresis loops provide the same kind of information; lowering the temperature causes the residual magnetization and coercitive fields to increase dramatically. The origin of this behavior is related to the blocking of the domain walls, as confirmed by the temperature dependence of the magnetization along the easy axis, which increases on decreasing temperature. The magnetization follows the law $M(T) = M(0) - aT^{3/2}$, expected for the spontaneous magnetization at low temperature of a single-domain three-dimensional ferromagnet.

In conclusion, the manganese–nitronyl nitroxide chains we have synthesized, showing very strong intrachain Heisenberg coupling, are extremely good one-dimensional ferrimagnets. On the other hand, they are not well suited as three-dimensionally ordered magnets, because the interchain interaction is essentially dipolar, and indeed the transition temperatures are similar to those observed in other one-dimensional ferrimagnets that have smaller intrachain but larger interchain interactions.[25] Better results can be obtained by exchanging the hfac molecules with other anions that can more efficiently transmit the exchange interactions between the metal ions.[38]

**Acknowledgment.** The financial support of the CNR and of the Italian Ministry of Public Education is gratefully acknowledged.

**Supplementary Material Available:** Table SI, containing crystallographic and experimental data for I and II, Tables SII–SV, listing anisotropic thermal factors and calculated positional parameters for I and II, and Tables SVI–SIX, containing bond distances and angles for I and II (13 pages); listings of observed and calculated structure factors for I and II (23 pages). Ordering information is given on any current masthead page.

(32) Nagata, K.; Tazuke, Y. *J. Phys. Soc. Jpn.* **1972**, *32*, 337.
(33) Karasudani, T.; Okamoto, H. *J. Phys. Soc. Jpn.* **1976**, *43*, 1131.
(34) Oshima, K.; Okuda, K.; Date, M. *J. Phys. Soc. Jpn.* **1976**, *41*, 475.
(35) Morrish, A. H. *The Physical Principles of Magnetism*; John Wiley & Sons, Inc.: New York, 1966.
(36) Renard, J. P. In *Organic and Inorganic Low Dimensional Crystalline Materials* Delhaes, P.; Drillon, M. Eds. NATO ASI SERIES; Plenum: New York, 1987.
(37) Villain, J.; Loveluck, J. M. *J. Phys., Lett.* **1977**, *38*, L77.
(38) Caneschi, A.; Gatteschi, D.; Renard, J. P.; Rey, P.; Sessoli, R. *J. Am. Chem. Soc.* **1989**, *111*, 785.